

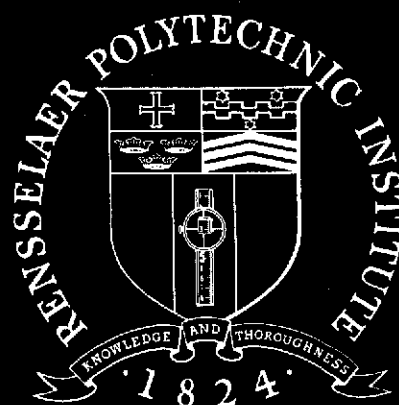
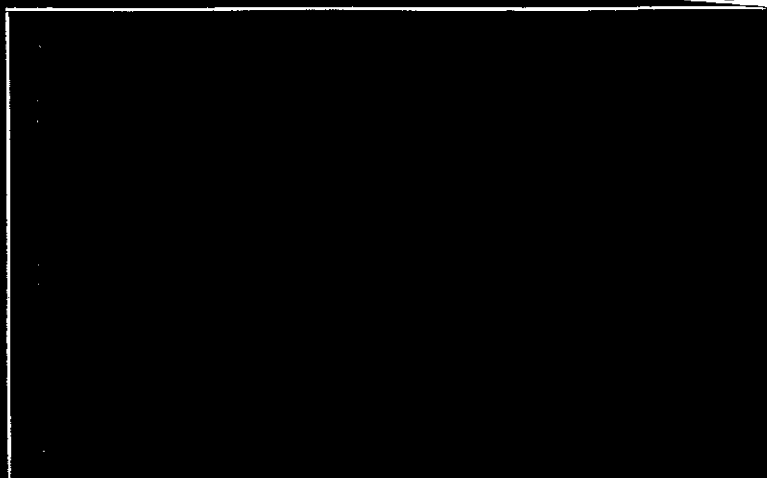
NASA-CR-136774) LASER SCANNING METHODS
AND A PHASE COMPARISON, MODULATED LASER
RANGE FINDER FOR TERRAIN SENSING ON A
MARS ROVING (Rensselaer Polytechnic Inst.)
51 p HC \$4.75

N74-16183

CSCI 20E

G3/16

Unclas
15916



Rensselaer Polytechnic Institute

Troy, New York

R.P.I. TECHNICAL REPORT MP-34

LASER SCANNING METHODS
AND
A PHASE COMPARISON, MODULATED
LASER RANGE FINDER
FOR
TERRAIN SENSING ON A MARS
ROVING VEHICLE

by
Glenn T. Herb

National Aeronautics and Space
Administration

Grant NGL 33-018-091

A project submitted to the Graduate
Faculty of Rensselaer Polytechnic Institute
in partial fulfillment of the
requirements for the degree of
MASTER OF ENGINEERING

School of Engineering
Rensselaer Polytechnic Institute
May, 1973

TABLE OF CONTENTS

LIST OF FIGURES	111
LIST OF TABLES	iv
ACKNOWLEDGMENT	v
ABSTRACT	vi
INTRODUCTION	1
PART I Laser Scan Methods	3
I-a Electro-Optics	4
I-b Converting Parallel Positions to Angles	17
I-c Scanning Systems	17
I-d Incident Spot Distortion	21
Part II Design and Implementation of a Laser Range Finder Using Phase Comparison Techniques	26
II-a Methods of Laser Rangefinding	26
II-b Maximum Modulating Frequency for a Modulated Laser - Phase Comparison Range Finder	27
II-c Improving Resolution with Heterodyning Techniques	29
II-d The Proposed Range Finder	30
II-e Instrumentation of the Rangefinder Electronics	40
CONCLUSIONS	43
REFERENCES	44

LIST OF FIGURES

	Page
1- Deflection in a binary crystal	7
2- Cascading binary deflection units	9
3- Background light vs. modulation voltage deviation	12
4- Angle generation with a simple lens	12
5- Kuriger scanning system	19
6- Proposed scanning system	19
7- Incident spot distortion	22
8- Proposed range finder	31
9- Range finder waveforms	34
10- Range finder output waveform	37
11- Effect of Schmitt trigger on noisy input	42

LIST OF TABLES

Table I- $\Delta\phi/\phi$ in % for several values of d and R

Page
25

ACKNOWLEDGMENT

The author wishes to express his gratitude to Prof. C. N. Shen for his advice, help, and understanding as faculty advisor during the preparation of this work.

ABSTRACT

Two areas of a laser range finder for a Mars roving vehicle are investigated: (1) laser scanning systems, and (2) range finder methods and implementation. Several ways of rapidly scanning a laser are studied. Two, digital deflectors and a matrix of laser diodes, are found to be acceptable. A complete range finder scanning system of high accuracy is proposed. The problem of incident laser spot distortion on the terrain is discussed. The instrumentation for a phase comparison, modulated laser range finder is developed and sections of it are tested.

INTRODUCTION

It is currently being assumed that a laser range finder type of sensor will be used to supply the terrain data used by the Mars roving vehicle during its autonomous navigation. This paper addresses itself to two areas of this sensor: (1) a laser scanning system, and (2) the range finder electronics and methods.

If the terrain data is to be collected as the vehicle is moving, the rocking and rolling of the vehicle as it travels the uneven terrain can be a large source of error. To attempt to reduce this error, the laser scan methods considered here are of a block scanning nature. That is, the entire field of view of the rover is scanned out very rapidly so that the rock and roll error between points is negligible and all points in the field may be considered to have been obtained simultaneously.

The criterion for a system worked under were:

1. No or few moving parts
2. An angle incremented scan (i.e. point spacings vary with distance from the vehicle)
3. Scan requirements- azimuthal angle 40° - 60°
range angle 40°

The last criterion results from the dimensions of the vehicle and the range of the scan (about 3 to 30 meters). The RPI vehicle is currently designed to be 10 feet wide,

or about 3.1 meters. To cover this width with a scan at 3 meters from the vehicle requires a 60° scan angle (i.e. $\pm 30^\circ$ from the direction of travel). To cover it at 5 meters requires a 40° scan angle.

Work was also done on instrumentation of the actual range finder. The method investigated was a phase comparison technique using an amplitude modulated laser beam as the probing element. This method has the advantage that the range information is contained in the relative phase of the modulation sinusoid waveform. Thus standard analogue filter techniques can be used on the detected return wave to improve its signal to noise ratio.

This paper is divided into two parts. The first part is a discussion of laser scanning methods. The second part deals with the range finder instrumentation.

PART I LASER SCAN METHODS

The first method looked at was a system using oscillating mirrors to do the sweeping. With this system it is very easy to synchronize the transmitter and the detector since both use the same optics. The transmitted pulse is fired, and the return pulse comes back through the optics 20 to 200 nano-seconds later. The mirrors have essentially not moved during this time and thus the detector is "looking" at the same spot at which the pulse was fired.

The problem with this system is that it uses oscillating mirrors from which the angle data must be taken. At the scan frequencies of interest (>10 KHz) angle decoders cannot be used on the oscillating mirrors because of the decoder disc's non-negligible inertia at those frequencies. Spinning poly-faced mirrors would solve the inertia problem, but synchronizing the two spinning mirrors with a high degree of accuracy and keeping them synchronized would be an extremely difficult task. It is therefore felt that this system would not be satisfactory.

In order to decrease or eliminate this necessity of detecting angle information from a mechanically oscillating mirror, it seemed that a reasonable approach would be to investigate electro-optic and other electronic scanners.

I-a Electro-Optics

There are several types of electro-optic devices.

The three considered were acusto-optic beam benders, piezo-electric deflectors and digital light deflectors.

Acusto-optic beam benders use the property of some crystals which causes their refractive index, n , to have a gradient proportional to a pressure gradient set up in the crystal. Therefore, since light is bent toward an increasing gradient in the refractive index, by changing the index gradient of the crystal the deflection of the beam is changed. In crystals which possess the acusto-optic property, the index gradient may be changed simply by changing the pressure gradient in the material. The major problem with this type of deflection, however, is that the proportionality constant between the pressure gradient and the n -gradient is extremely small [1]. Since the actual scan angle is related to the index gradient by the approximation:

$$\theta' = L (dn/dx) \quad (1)$$

where θ' = the deflection angle

L = the length of the crystal in the direction of propagation

dn/dx = the index gradient normal to the direction of propagation

a small proportionality constant between dp/dx (the pressure gradient) and dn/dx will result in a very small scan angle for practical values of L . As an example, typical commercial units provide deflection angles on the order of tenths of degrees. These angles are much too small for our purposes.

Piezoelectric deflectors use the well known piezoelectric effect of certain crystals which causes them to deform in certain ways when an electric potential is applied across them. The most common deformation used are the longitudinal and the shear deformation. A reflective surface is attached to one face of the crystal, and it is the motion of this surface as the crystal is deformed which is used to cause the deflection.

The advantages of this type of deflection is that the transmitted light pulse and return pulse may use the same optics. It thus has all the advantages of the vibrating mirror scan described earlier without the problems associated with the mirrors being mechanically scanned and synchronized. But once again maximum angle is limited. Commercially available units have maximum scans on the order of 6° [2]. Also the angle data must be obtained indirectly from the analog control voltages.

Digital deflectors are sensitive to the incident light's direction of polarization. The incident beam will be laterally displaced or angularly deflected to one of two possible positions depending on its direction of polarization.

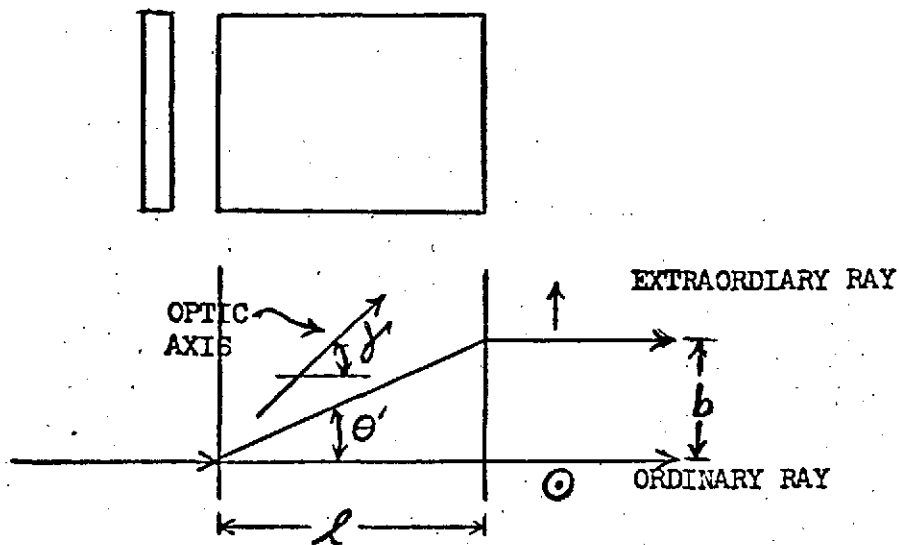
These deflectors consist of a polarization modulator, such as a Pockel or Kerr cell, which either rotates the direction of polarization 90° or allows it to pass unrotated, followed by a binary birefringent discriminator, i.e. a crystal with two indices of refraction depending on the direction of polarization of the incident light. The number of positions available at the output of a deflection system can be increased by cascading individual binary units. Properly cascading N of these units results in 2^N positions in the final output. Going from a one dimensional to a two dimensional scan is easily accomplished by adding an M unit scanner rotated by 90° with respect to the first N units. This results in an array of 2^N by 2^M possible deflection positions.

The binary units accomplish a lateral displacement as shown in figure 1 [3]. An incident beam of collimated light will be deflected by an angle θ if its polarization direction is in the plane of the crystal's optical axis. If the direction of polarization is normal to the plane of the axis, the beam is not deflected at all. When the deflected beam hits the edge of the crystal, it is again deflected so that it emerges from the unit parallel to the incident beam. Therefore a two dimensional digital scanner will provide a 2^N by 2^M matrix of parallel beam positions. A method of converting these parallel beam scans into angular scans will be covered later in section I-b.

The angle θ' is a function of the crystal material and

Figure 1

DEFLECTION IN A BINARY CRYSTAL



MATERIAL	θ' IN DEG.	γ IN DEG.	for $\lambda = 6328 \text{ \AA}$ (He-Ne)
NaNO_3	9.17	49.34	
CaCO_3	5.90	51.27	
KH_2PO_4	1.48	53.87	

the angle the optic axis has with respect to the incident beam. The figure also gives maximum values of θ' for three crystal materials and the value of γ needed to obtain that maximum.

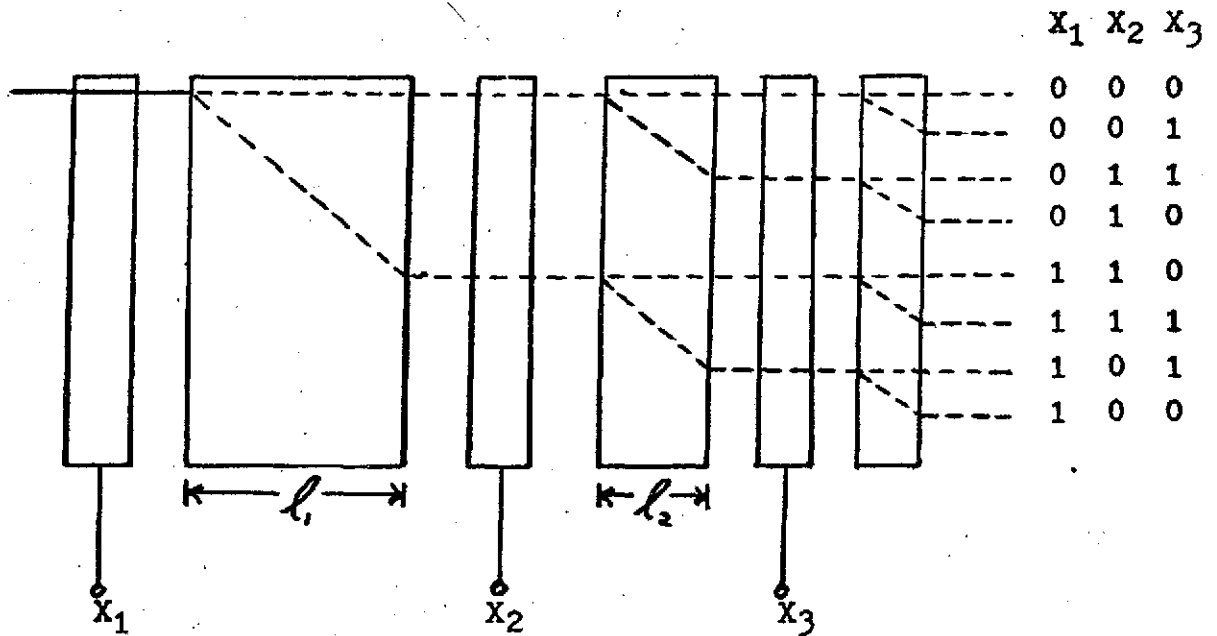
Note that in each cell the control voltage is either present or absent, corresponding to either a rotated polarization in that cell or a non-rotated polarization. Therefore, each position available at the output can be associated with a unique binary code word determined by which cells are energized and which are not for that point. Thus each point in the sweep is known exactly by the particular code word being issued by the control logic at that instant.

Proper cascading of the binary units to obtain a 2^N point array is accomplished by maintaining the proper relation between the lengths of the birefringent crystal in the cascaded units. Since each crystal produces the same internal deflection angle if the incident light is polarized in the plane of the crystal's axis, and no deflection if it's polarization is normal to the axis, the crystals cannot be of constant length. Figure 2 shows the proper cascading. It can be seen that in order for each crystal to produce a new position for every beam incident on it, its length, ℓ , must be half of its immediate predecessor's. Therefore, the length of the j^{th} crystal in the cascade must be:

$$\ell_j = \left(\frac{1}{2}\right)^{j-1} \ell_1 \quad (2)$$

Figure 2

CASCADING BINARY DEFLECTION UNITS



$X=1 \Rightarrow$ Polarization Rotated

$X=0 \Rightarrow$ No Rotation

Note position labels form a 'cyclic' binary code

There are several problems with these binary units, however. To rotate the polarization of light by 90° in a Pockles cell, the half wave voltage must be applied to the cell in such a way as to set up an electric field in the cell parallel to the direction of light propagation. To accomplish this, electrodes must be placed in the optical path. This then creates the problem of finding the optimum compromise between the two competing requirements of low resistance electrodes and maximum transmittance of light by the electrodes. Kulcke found highly acceptable results could be obtained using a variety of electrode - adhesive combinations [3]. It was also found that the modulator electrode transmittance was the limiting factor and hence the total system transmittance could be approximated as

$$T_{\text{sys}} = t^{2n} \quad (3)$$

where t is the transmittance of an electrode - adhesive combination, and n is the number of cells in the system ($2n$ appears because there are two electrodes per modulator).

Another problem of discriminator cells is background light, that is light appearing at a point or points other than the one called for. The major cause of this is deviation of the modulator's control voltage from the required half wave voltage. As the control voltage becomes greater than or less than the half wave voltage, the polarization of the light is rotated more or less than 90° . It will then

have a component in the unrotated direction. The two components will be split by the discriminator crystal and the undesired component will appear as ghosting at the un-called-for position. Values of this background light have been graphed [3] and are shown in figure 3. Note that the background light can be kept below the incident light by more than 40 db if the voltage deviation is kept below 10%, a tolerance which is easily obtained with a good regulator circuit.

There also exists a problem due to the fact that all the points in the NxM position matrix at the output of the deflector do not represent the same path length through the deflector. This can be easily seen by referring back to 2. This difference in path length, and therefore time, for the laser beam to get to the transmission plane of the deflector could cause problems in the actual rangefinder instrumentation if it is not compensated for. If a plane was located parallel to the transmission plane of the deflector, and if its distance from the actual laser was defined to be a certain path length of an undeflected beam (e.g. path 000 in figure 2), then that same path length taken on all the other beam positions would fall short of this plane by some amount ΔZ . It can be shown [4] that these differences in distances from the laser for the same path length can be expressed as

Figure 3

BACKGROUND LIGHT vs. MODULATOR
VOLTAGE DEVIATION

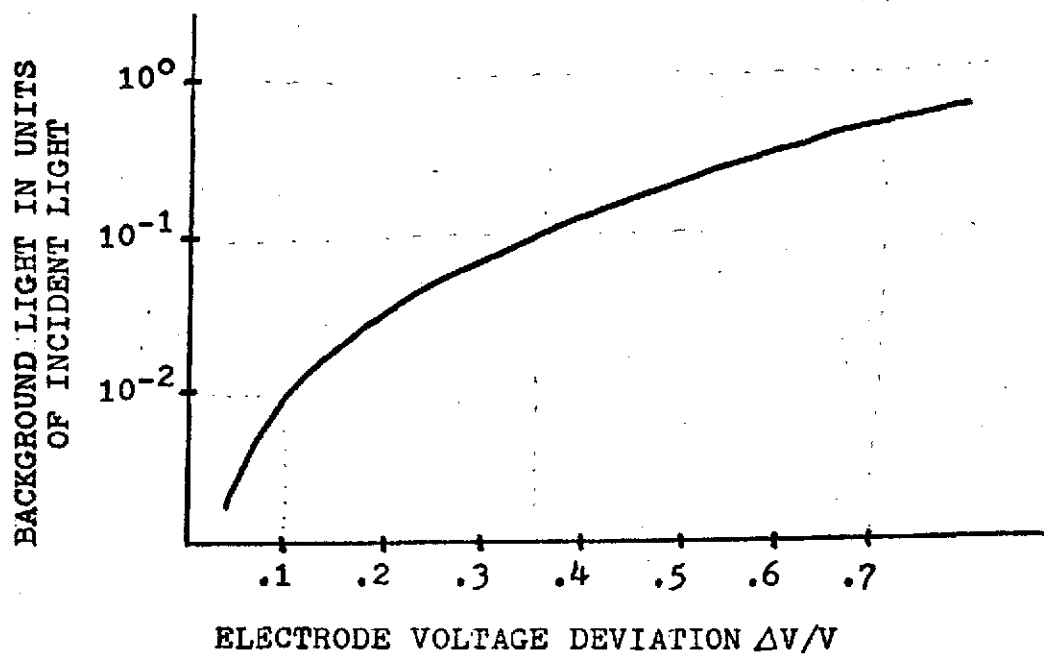
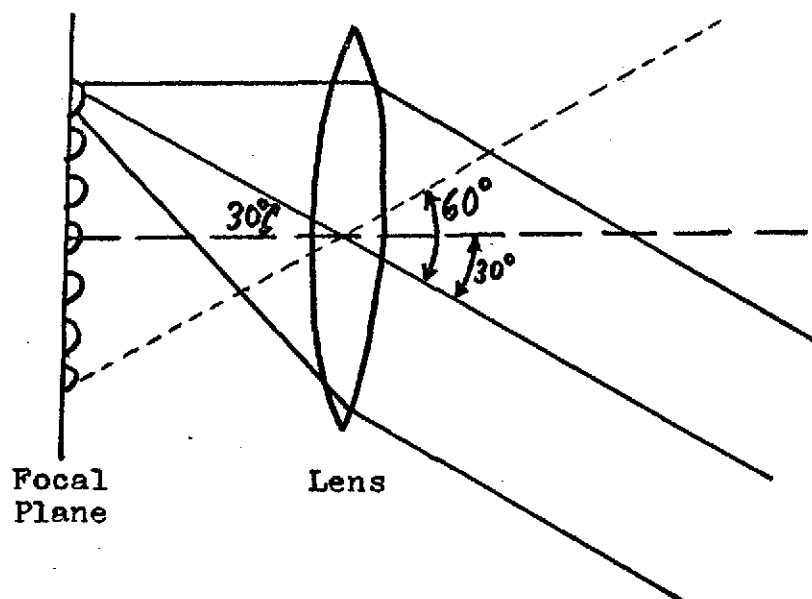


Figure 4

ANGLE GENERATION WITH A SIMPLE LENS



$$\Delta Z = (Z_d - Z_o) = \left(\frac{n}{n_r^2} - \frac{1}{n_o} \right) \cot \theta' (dx + dy) \quad (4)$$

where: Z_d = the distance from the laser to the fixed path length position of the deflected beam.

Z_o = the distance from the laser to the fixed path length position of the undeflected beam (i.e. the reference plane)

dx and dy = the x and y displacements of the beam relative to the undeflected beam

θ' = the internal deflection angle within a crystal undergone by an extraordinary ray (refer to figure 1)

n_o = the index of refraction of a crystal for an ordinary ray

n and n_r^2 are dependent on both the ordinary and extraordinary indices of refraction. Explicitly:

$$n = \left(\frac{n_o^2 + n_e^2}{2} \right)^{\frac{1}{2}} \quad (5)$$

and

$$n_r^2 = \frac{2n_o^2 n_e^2}{(n_o^2 + n_e^2)} \quad (6)$$

where n_e = the index of refraction of a crystal for an extraordinary ray.

If we take the worst case, i.e. if γ in figure 1 is adjusted

so $\theta' = \theta'(\max)$, it can also be shown that

$$\cos \theta'(\max) = 2n_e n_o / (n_o^2 - n_e^2) \quad (7)$$

If we now substitute equations (5), (6), and (7) into equation (4), we obtain

$$\Delta Z = \frac{n_o(n_o^2 + n_e^2)^{3/2} - \sqrt{2}(2n_o^2 n_e^2)}{\sqrt{2} n_o^2(n_e)(n_o^2 - n_e^2)} (dx + dy) \quad (8)$$

Since for a given crystal and a given laser frequency n_o and n_e are constants, the entire first term of the above is a constant. Hence, equation (8) can be rewritten as

$$\Delta Z = Kdx + Kdy \quad (9)$$

But this is just the equation of a plane, and hence we have found that the phase difference caused by unequal path length through the deflector can be easily compensated for. The computer on board the rover will know which position was transmitted and would then be able to subtract this pre-determined range error associated with that particular point.

The advantage of this system is that the positions and therefore the scan angles transmitted are known exactly. A position is called for by the scan logic and that scan angle (both horizontal and verticle angles) is produced. Therefore, no indirect measurement is needed, and the associated error is thus eliminated. The disadvantages are its relative bulk, and the large voltages required (the half wave voltage

of a Pockels cell is on the order of a kilovolt). Also the return beam cannot use the same optics.

Power dissipation for this type of deflector can be estimated by investigating the polarization modulators used. If we consider using a Pockels cell of KH_2PO_4 as our modulator, we can use the known [4] approximate dissipation equation

$$W_{\text{dis}} \approx (0.938 + 1.94 \times 10^{-3} T) \times 10^{-6} \left(\frac{a b}{c} \right) \frac{\text{joules}}{\text{cell/cycle}} \quad (10)$$

where: W_{dis} = the dissipated energy per cell per cycle

T = the temperature above the cell's Curie temperature

a , b , and c = the dimensions of the cell in the horizontal, vertical, and direction of light propagation, respectively

For an $N \times M$ matrix of positions, we will have $N \times M$ Pockels cells. But since the positions are called for in a Gray code order (recall figure 2), only one cell is switched at any time, and the switching frequency of the cells goes down as their "significance" in the Gray code word goes up. Hence total power dissipation will be

$$\begin{aligned} P_{\text{dis}} &= W_{\text{dis}} \frac{1}{2} f_s + W_{\text{dis}} \frac{1}{4} f_s + \dots + W_{\text{dis}} \left(\frac{1}{2} \right)^{n-2} f_s + W_{\text{dis}} 2 \left(\frac{1}{2} \right)^{n-1} f_s \\ &= W_{\text{dis}} \left(\frac{1}{2} + \frac{1}{4} + \dots + \left(\frac{1}{2} \right)^{n-2} + 2 \left(\frac{1}{2} \right)^{n-1} \right) f_s \end{aligned} \quad (11)$$

where f_s = the position switching frequency, and $n = N+M$.

But the series in brackets in equation (11) is always equal to unity. Hence

$$P_{dis} = W_{dis} f_s \quad \text{watts} \quad (12)$$

An alternative to the digital deflector optics is a matrix of N by M individual laser diodes. This has all the advantages of the binary deflectors, but lacks the problem of high voltages and is somewhat less bulky. In addition, this type of system offers the option of predistorting the matrix. That is, if a non-uniform matrix of scan locations on the terrain is desired, or if a data point layout other than the equal angle incremented scan is wished to be simulated, the individual diodes can be shifted around on the transmission plane of the scanner. This pre-distorted matrix when passed through the angle generating optics described in the next section, will result in the desired non uniform scan.

A very important advantage of this system is that the laser duty cycle of the entire system can be quite high while keeping the duty cycle of the individual laser diodes quite low. For example, if it takes one millisecond to interrogate a data point and if a grid of 500 data points is interrogated once every 5 seconds, the system laser duty cycle will be 10%, while the individual diodes' duty cycles will be a much more realistic .02%.

The disadvantage of this type of system is that it

requires N times M diodes whose alignment is critical. In addition, only semiconductor lasers can be practically used.

I-b Converting Parallel Positions to Angles

The last two methods both provide parallel light outputs. This must be converted to scan angles if the method is to be useful in a scanning system.

This can be accomplished by placing the origin of the parallel positions on the focal plane of a small aperture lens. This is shown in figure 4 for the case of a matrix of laser diodes, i.e. uncollimated light. The case of binary deflection optics with collimated light is similar except that instead of collimating, the lens simply deflects the beam almost as if it were an ideal "ray".

I-c Scanning Systems

One possible system, the dual vibrating mirror scan, was mentioned earlier in this paper. Here, two more systems will be introduced which attempt to alleviate the problems of the dual mirror approach.

Kuriger [5] has worked on and proposed a hybrid scan system using a vibrating mirror for a vertical scan and a line of laser diodes to accomplish the horizontal scan. His range finder system is not capable of producing the necessary accuracy, but his scanning system does have some advantages. Kuriger's system is presented with some minor

modifications in figure 5. The "pulse transmitted detector" has been added to conform with the information needed in one of the range finding schemes currently under study. In this system both the transmitter and the detector use the same verticle scan mirror. The diodes provide the horizontal scan, while the receiver looks at the entire horizontal scan area via the cylindrical lens. The use of the same scan mirror assures synchronization between transmitter and reciever, and the narrowing of the detector's field of view to only one horizontal row at a time increases the signal to noise ratio. Further advantages of this system are its compactness and small number of components. But although the horizontal transmitted angle is known exactly, the verticle angle determination relies on the same type of mirror position detection as does the dual mirror system and suffers the same problems.

An alternative system which seems to avoid all the major scan problems is now presented. Figure 6 shows the proposed system using digital deflection optics, but a matrix of laser diodes could be substituted just as well.

The detection system used is similar to Kuriger's except the detector section is mechanically a separate entity from the transmitter. When the mirror drive starts its verticle sweep, the synch (start) circuit detects this and initiates the transmitter's scan. The transmitter's verticle scan is approximately synchronized to the mirror,

Figure 5
KURIGER SCANNING SYSTEM

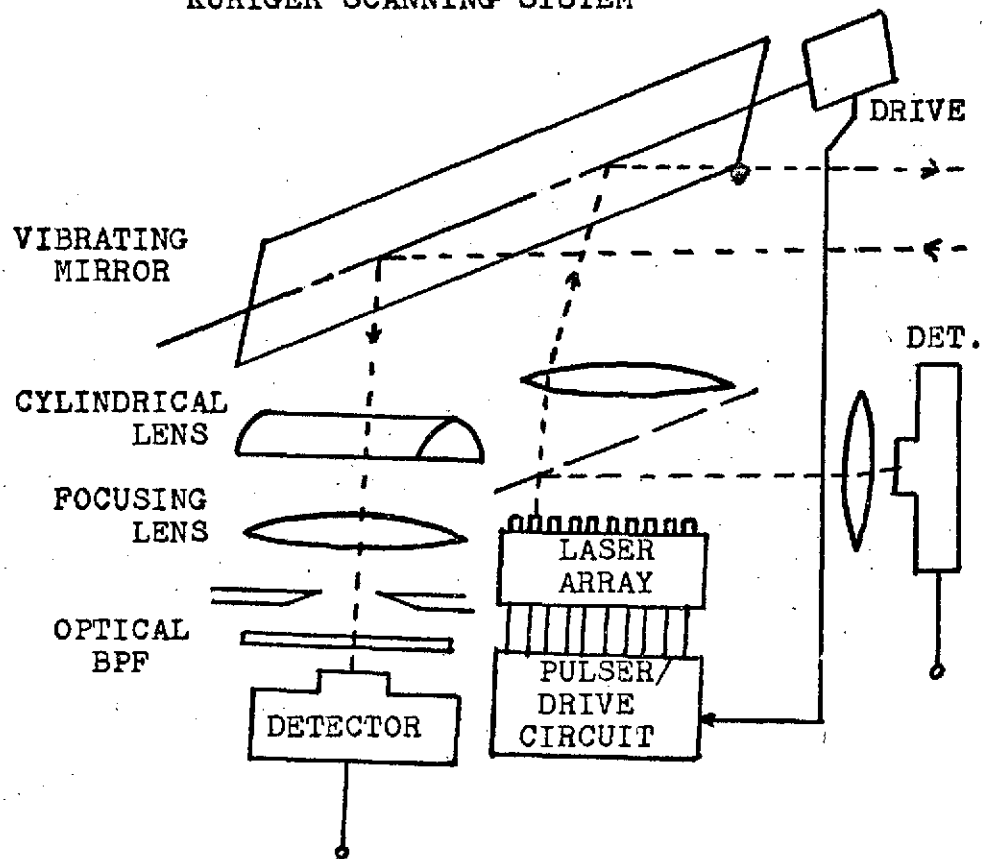
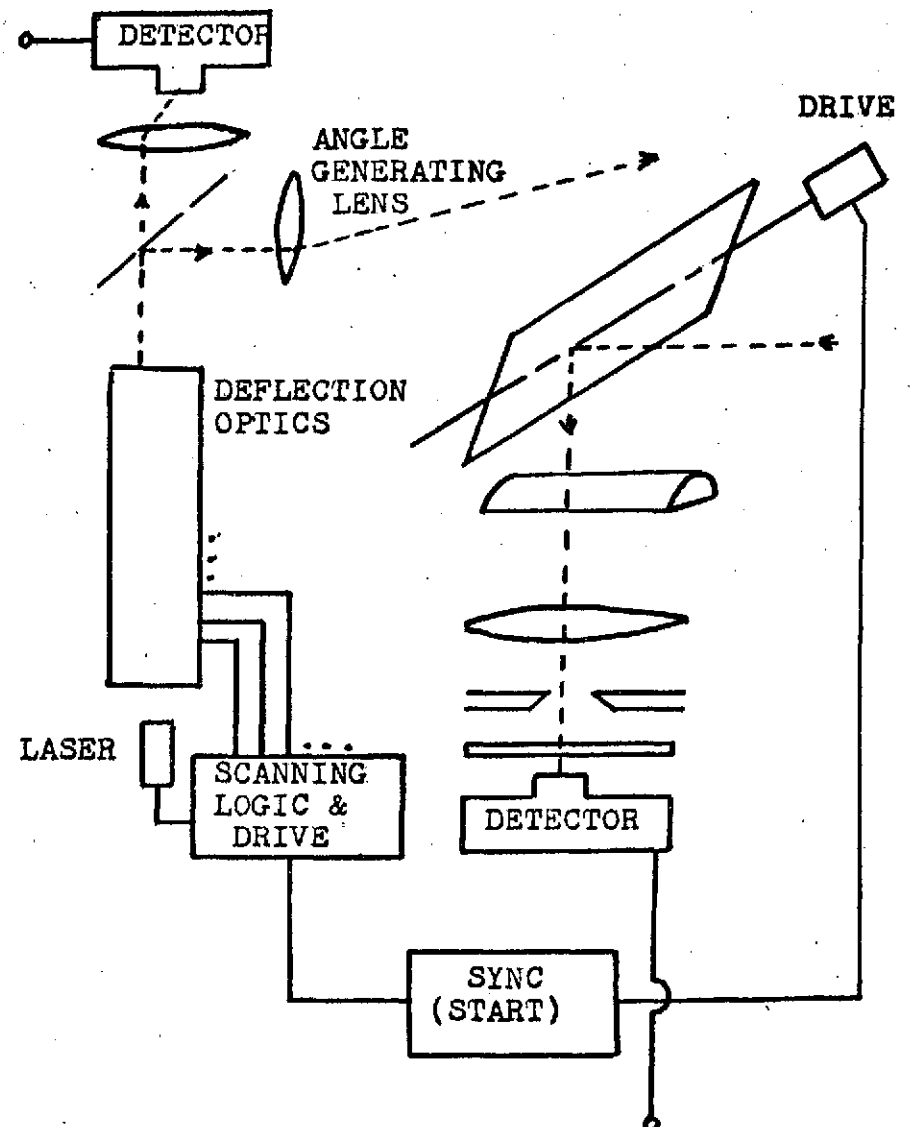


Figure 6
PROPOSED SCANNING SYSTEM



but the detector is given a wide enough field of view to compensate for a slight mis-match. Any mis-match which does occur does not continue to accumulate since the transmitter and detector are re-synchronized at the beginning of each vertical scan.

The advantages of this system are many-fold. First, the actual laser scanning is completely solid state. Also the transmitted angles are known exactly, with each pair of horizontal and vertical having its own binary code label. Finally, although a hybrid detector scheme is used, data point accuracy is extremely improved because we are not relying on the mirror position to give point location, only to narrow the detector's field of view to the approximate azimuthal scan line of the transmitter. This system then seems to have the potential for extremely accurate transmitted angle information while maintaining a reasonable signal to noise ratio at the detector by narrowing its field of view.

The maximum scan angle obtainable with this system is determined by the angle generating lens system used. For the single lens set up shown in figure 3, maximum scans of 55° can be obtained with a good lens. If a multiple lens system is used, this "viewing angle" can be greatly extended from this maximum. For example, using standard photographic lenses as a guide, a 28 mm focal length lens (6 elements) has a viewing angle of 74° , a 20 mm lens (11 elements) has a

viewing angle of 94° . If distortion of field is allowed (an effect which can be compensated for by appropriate placement of beam sources on the matrix plane) fisheye lenses can also be used. Fisheye lenses have viewing angles from 180° (10 mm focal length) to 220° (6 mm focal length).[6]

Since all lenses are circular, the angle maximum is completely symmetric with respect to the optic axis and therefore holds for both azimuthal and range angles.

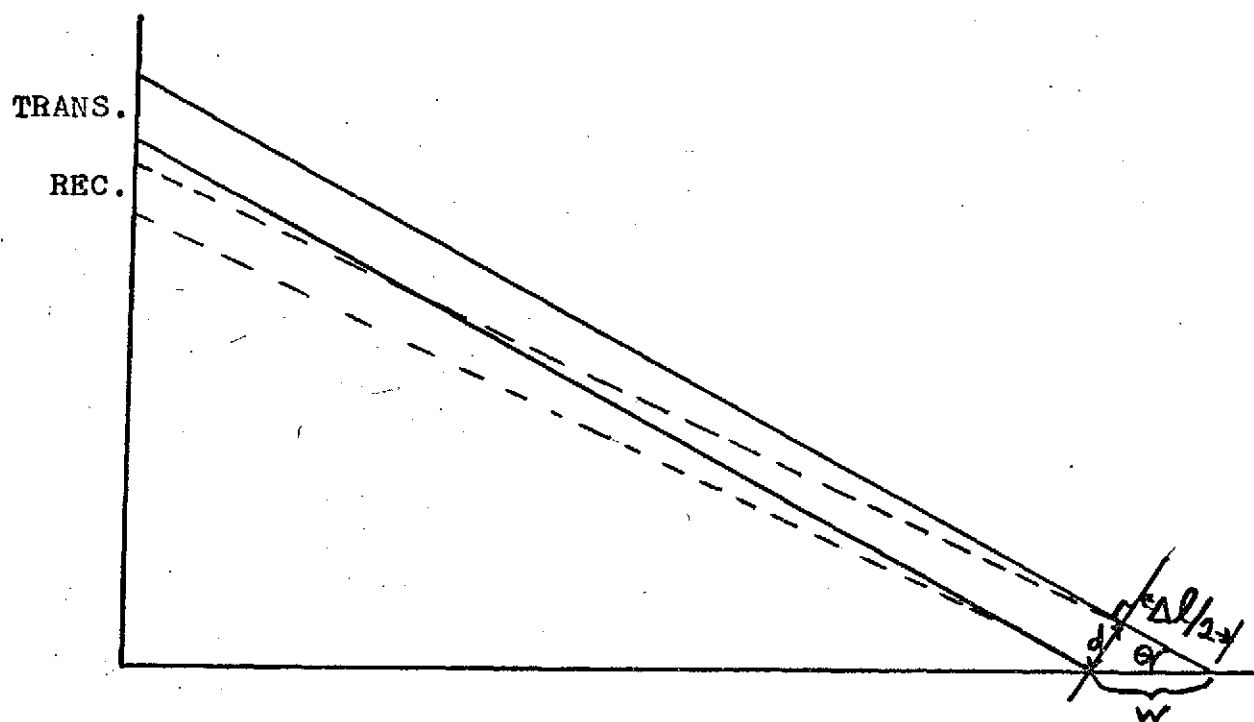
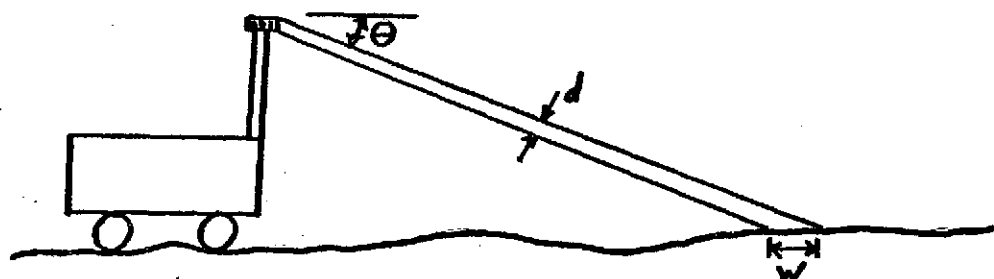
Scan rate is limited only by position switching time. For the case of a matrix of laser diodes, minimum switching time is caused by the diodes' minimum pulse width and the maximum usable frequency of the driver circuits. This is on the order of magnitude of 100 KHz or 10 microseconds per position. Thus the limiting factor for sweep rate will not be the scan unit, but rather the minimum on-time of the laser needed by the range finder system. This will be much larger than 10 micro seconds.

For a matrix of diodes system the weight of this scan mechanism will most likely be under 10 pounds.

I-d Incident Spot Distortion

One problem with all the angular scan methods is the incident spot distortion at the terrain. Since a collimated beam is transmitted at an angle, the actual shape and size of the spot will be distorted when it strikes all surfaces other than those to which it is normal (see figure 7). This

Figure 7
INCIDENT SPOT DISTORTION



is most severe at the maximum ranges. As can be seen from the figure

$$W = \frac{d}{\sin \theta} \quad \begin{array}{l} \text{for horizontal terrain} \\ \text{(i.e. in the plane of the rover)} \end{array} \quad (13)$$

Therefore, at 30 meters ($\theta = 5.7^\circ$) a 2.5 cm beam diameter ($\cong 1$ inch) would produce a spot length of 25 cm. This effect worsens for negative in-path slopes and improves up to a point for positive in-path slopes.

This distortion results in different rays within the beam traveling different total paths. Thus a ray on the top of the beam in figure 7 would travel a total round trip distance of $2x(\Delta l/2)$ or Δl more than a ray on the bottom of the beam. This distribution of path lengths within a single beam will cause a time of flight ambiguity at the range finder's detector. In the case of a modulated beam type range finder (which is described more fully in Part II), the phase of the modulating frequency on the returning beam relative to the outgoing beam is what supplies the range information. Spot distortion will cause a phase blur of a magnitude proportional to the amount of distortion. Referring to figure 7, we can show that (taking the speed of light to be 3×10^8 meters/second)

$$\Delta\phi = .024f_m (w^2 - d^2)^{\frac{1}{2}} \quad (14)$$

where $\Delta\phi$ = peak to peak phase blur in degrees

w = incident spot length in cm.

d = beam diameter in cm.

f_m = modulating frequency in MHz

But since

$$\phi = (\Delta t) f_m 360^\circ \quad (15)$$

where ϕ = relative receiver to transmitter phase of modulating frequency

Δt = beam ideal round trip transit time in microseconds

we see that the error introduced by the phase blur is

$$\frac{\Delta\phi}{\phi} = \frac{.024}{360} \frac{(w^2 - d^2)^{\frac{1}{2}}}{\Delta t} \quad (16)$$

Note that equation (16) is independent of f_m . Therefore, the phase blur error is independent of the beam's modulating frequency. It is therefore free to be chosen by other constraints.

Table I shows values of $\Delta\phi/\phi$ as a function of range in front of the vehicle, R , and beam diameter, d . This can be done since R is a function of θ and w is a function of d and θ (recall equation 13). Note that the errors introduced by spot distortion on a flat terrain are negligably small over a large range of d (the accuracies desired are in the range of .1% to 1% - see section II-c).

TABLE I

<u>R</u>	$\Delta\phi/\phi$ in %		
	<u>d=.5</u>	<u>d=1</u>	<u>d=2</u>
3	.0131	.0262	.0524
5	.0158	.0317	.0635
10	.0178	.0355	.0709
20	.0183	.0366	.0732
30	.0134	.0368	.0737

PART II DESIGN AND IMPLEMENTATION OF A LASER RANGEFINDER USING PHASE COMPARISON TECHNIQUES

II-a Methods of Laser Ranging

The simplest type of laser ranging is the timed pulse method. The laser is simply pulsed for a very short time and the detector watches for the reflected return pulse. The time between the pulse's transmission and its detection is then timed and this time of flight information is converted to range data.

An alternate method is the modulated laser beam-phase comparison method. In this scheme the laser is amplitude modulated with a high frequency. This necessitates a much longer laser pulse than the previous method since the laser's unmodulated component of power output must reach a steady state value and stay there long enough for good data to be obtained.

The detector receives the reflected laser's output. The radio frequency modulating signal is then removed from the detected signal and put through a very narrow band (high Q) band pass filter. This very high Q filter tends to block the large amount of noise that will be imposed on the laser signal in the process of its bouncing off the terrain.

The processed RF signal is now phase compared with the source which is providing the modulating frequency. Since the return signal has gone through a longer path than the source

signal in getting to the phase comparator, it will be delayed in phase by an amount proportional to that increased path length. Hence, the detected phase difference is proportional to the range as seen by the laser.

The ability to use common and relatively simple analog filters to obtain a great increase in signal to noise is one of the major reasons that this method seems so promising. In the timed pulse method, on the other hand, a noisy returned pulse will cause a large problem in deciding when to stop the time of flight counter. But since the noise also severely distorts the pulse's shape, there is no easy filtering scheme that can be employed to improve the signal to noise ratio. The modulation scheme does, however, require a longer laser pulse width than the timed pulse method. Therefore, it will require more power, but in return one obtains the signal to noise ratio improvement desired with more ease. The rest of this paper deals solely with the modulation method of range finding.

II-b Maximum Modulating Frequency for a Modulated Laser - Phase Comparison Rangefinder

The modulation frequency of the laser is determined by the ranges of interest (recall it was shown in section I-d that our choice of frequency is not constrained by spot distortion/ phase blur requirements). The phase delay introduced into the modulating frequency due to the

path length of the laser must not be allowed to become greater than or equal to 360° since, for example, 370° is ambiguous with 10° , etc. This requirement implies that our maximum frequency will be set by the maximum range. Recalling equation (15) and solving it for f_m , we have

$$f_m = \frac{\phi}{(\Delta t)360^\circ} \quad (17)$$

To find the upper limit on f_m , we set $\phi = 360^\circ$. Therefore:

$$f_m(\max) < \frac{1}{\Delta t_m} \quad (18)$$

where Δt_m = the maximum round trip transit time of the laser beam.

$$\text{Since} \quad \Delta t = 2R'/c \quad (19)$$

where R' = the actual one way path length of the laser beam

c = the speed of light,

we can estimate a maximum frequency by noting that at large ranges in front of the vehicle, the horizontal range from the vehicle, R , is approximately equal to R' . At $R = 30$ meters this is a good approximation (for a mast height of 3 meters). Therefore, our maximum frequency is

$$f_m(\max) \frac{1}{2(30)/3 \times 10^8} = 5 \text{ MHz.} \quad (20)$$

II-c Improving Resolution with Heterodyning Techniques

The accuracy we are looking for is on the order of ± 1 cm in the mid range of the scanning field (3 to 30 meters). This scanning field corresponds to round trip times of approximately 20 to 200 nanoseconds and the accuracy requirement calls for a resolution on the order of .1 nanoseconds. This resolution is extremely difficult if not impossible to attain using current technology and considering the device's working environment. But remember these times are represented by phase differences between the return signal and the "in house" or modulating signal. These phase differences range from 0 to 360 degrees. From elementary modulation theory, it is known that if two sinusoids of different frequencies are multiplied together, one of the components of the resultant output is a sinusoid whose frequency is the difference of the two original inputs. Also, if one of the two original inputs has a constant phase term, this term will be maintained and the lowest frequency component of the output will be the difference frequency with a constant phase angle equal to the input angle, i.e. $\sin [(\omega_1 - \omega_2)t + \phi_1]$.

This effect proves very useful in expanding the time base of the information carrying phase angle of the return signal of the laser. For example, one way of comparing phase is to check corresponding zero crossings of two signals and see how far behind one lags the other. For a 1 MHz

modulation frequency say the return beam has experienced a 45° phase delay with respect to the "in house" reference signal. Using the zero crossing method, a 45° delay at 1 MHz means that the return signal will lag by 125 nanoseconds. If before the phase comparison is done, however, both the returned signal and the in house reference signal are heterodyned to some lower frequency, the phase difference between them will be preserved, but the time between respective zero crossings will have been expanded. In the example cited above, if the 1 MHz signals are heterodyned down to 10 KHz, the 45° phase difference will be maintained, but 45° at 10 KHz using the zero crossing method means that the return signal will lag by 12.5 microseconds. Therefore, heterodyning the signal down by a factor of 100, results in expanding the phase difference in time by a factor of 100. For a given system clock frequency, we have, therefore, increased our resolution by 100 times.

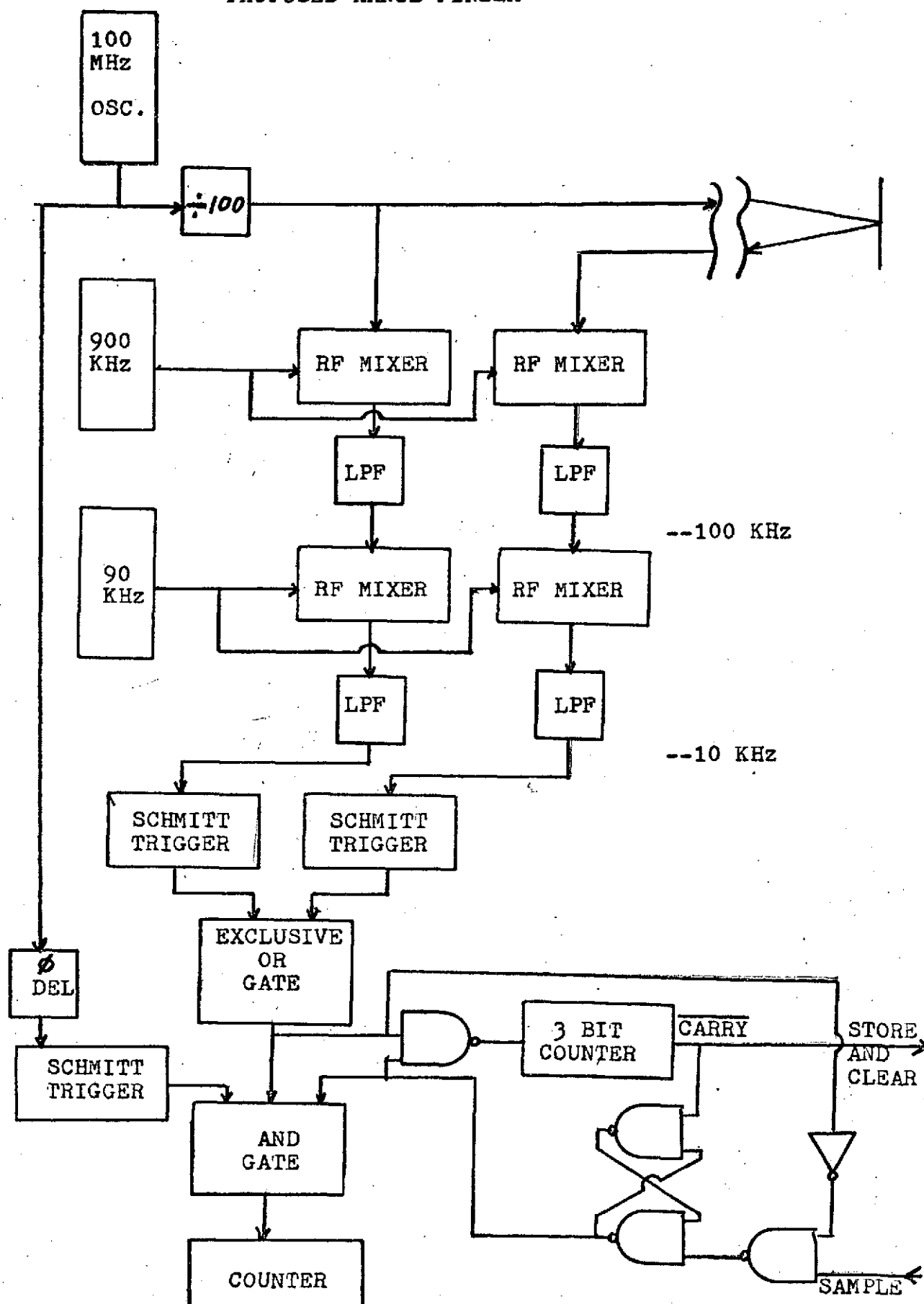
This heterodyning scheme is used in the proposed range finder design which is described in the next section.

II-d The Proposed Range Finder

A block diagram of the proposed range finder electronics is shown in figure 8. A 1 MHz main oscillator has been illustrated, but recall from section II-b that we may theoretically use up to a 5 MHz oscillator. The actual laser modulator and detection circuits are indicated by the

Figure 8

PROPOSED RANGE FINDER



broken line at the top of the page. It is also assumed that the signal enhancing and filtering described in section II-a has been incorporated in the detection circuits, and the returned signal input to the shown system is this preprocessed signal.

The heterodyning method of resolution expansion described in the previous section is incorporated here and is shown as a two step downward frequency translation by a factor of 100. The two steps are used to provide more stability. Since the down converting is a subtraction process, and subtraction of two large numbers which are close in magnitude tends to be a major error source, multiple stage down converting helps to provide greater stability in the final output frequency.

Note that both the returned signal and the in house reference signal go through the same processing. This is done to ensure that the phase difference that exist before the heterodyning is the same phase difference that exists after the down converting. By heterodyning both signals simultaneously, any phase error which is introduced by any of the local oscillators (the 900 KHz and 90 KHz sources in the figure) is added to both the returned and reference signals. Therefore, the phase difference between them remains the same. The low pass filter (LPF) following each mixer passes only the lowest frequency component of the mixer output which is the desired difference frequency.

The two down converted signals (now at 10 KHz in the figure) are then put through Schmitt triggers which converts them both to square waves and prepares them for the digital phase comparator. The Schmitt trigger is a threshold device, and the threshold and hysteresis may be set to any desired value. In the following it has been assumed that the thresholds have been set at zero with no hysteresis. This assumption is for ease of analysis only, and it is not suggested to actually use these settings. More realistic choices of thresholds and hysteresis are discussed in section II-e.

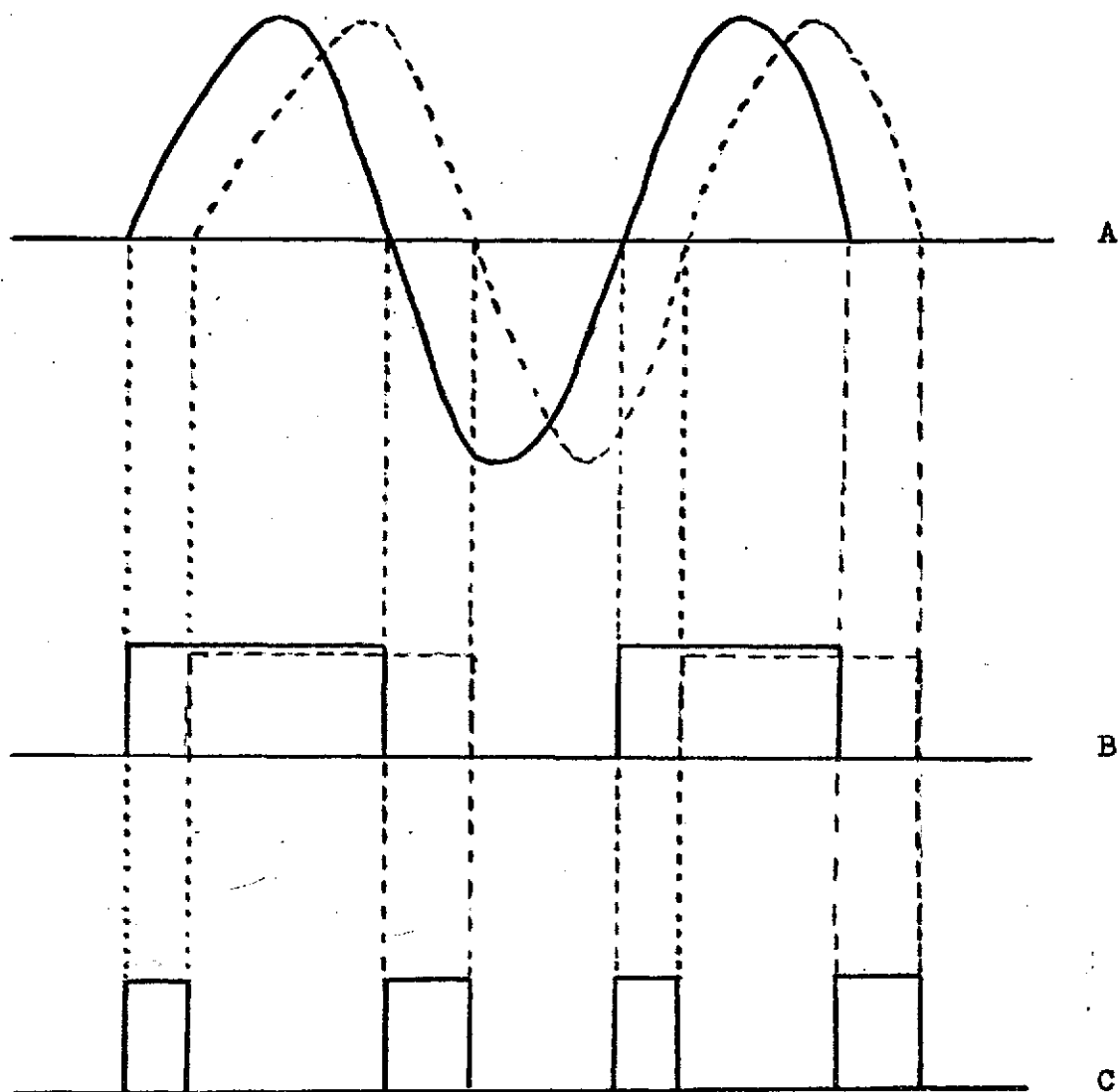
The outputs of the Schmitt triggers under the above assumptions are shown in figure 9-B.

These squared wave forms are then put into an exclusive OR gate. An exclusive OR gate has the property that its output will be "1", or high, if one or the other, but not both, of its inputs are high. The output will be "0", or low, otherwise. The truth table for such a gate is:

A	B	Q
0	0	0
0	1	1
1	0	1
1	1	0

where A and B are inputs and Q is the output. Therefore, we see from figure 9-C that if the Schmitt outputs are fed into the exclusive OR gate, the output will be a pulse whose width is proportional to the phase difference between

Figure 9
RANGE FINDER WAVEFORMS



Key to A and B

—— in house reference signal
----- returned signal

the squared in house reference signal and the squared return signal. This pulse contains the desired phase (and therefore range) information that is being sought.

To extract the phase information from this pulse, its length must be determined. To do this digitally, the pulse must be timed by a system clock. Recalling figure 8, we note that the 1 MHz modulating frequency was obtained by counting down by 100 from a 100 MHz master oscillator. This 100 MHz source frequency (which will be in phase with the 1 MHz modulation frequency) can then be used as a system clock. The frequency is then put through a sine to square wave converter or a Schmitt trigger and the resulting square waves are used to time the exclusive OR output pulse.

One section neglected in the above paragraph is the phase delay (ϕ DEL) block shown in the master clock's path in figure 8. This is added to take advantage of the fact that the clock frequency and the modulating frequency are initially in phase. Since the modulating frequency has gone through the heterodyning equipment, it has experienced a phase delay with respect to the master oscillator at the point where it enters the Schmitt trigger. To compensate for this delay and bring the two frequencies back in phase again, the phase delay block is added in the master clock's path. This delay is adjusted so that it equals the delay introduced by the heterodyning path.

The advantage that is obtained by having the system clock

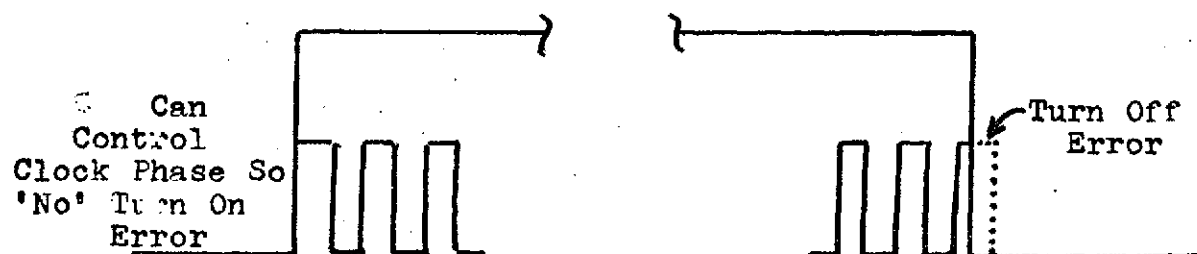
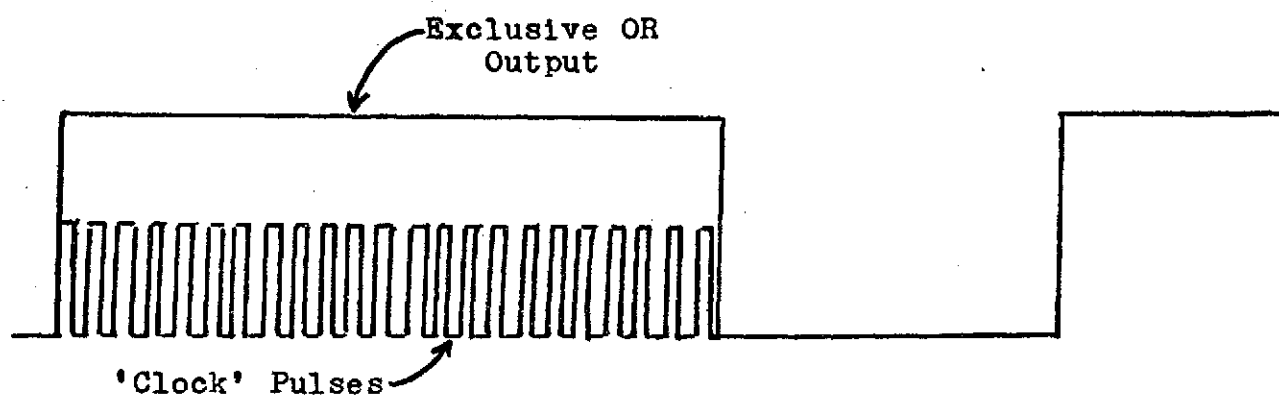
and the down converted modulation frequency in phase can be seen by referring to figure 9. Note that the leading edge of the exclusive OR gate output in 9-C is always caused by the leading edge of the modulating or in house reference frequency. Therefore, if the clock pulses' leading edges are in phase with the modulating frequency's leading edge, the leading edge of the phase information carrying exclusive OR pulse will coincide with the leading edge of a clock pulse. This implies that there will be no within-clock period resolution, or quantization, error at the leading edge of the phase pulse. Figure 10 shows this diagrammatically. This locked leading edge scheme provides a substantial improvement over the free running clock method. The maximum timing error using the locked system is $\pm T/2$ compared with $\pm T$ (where T is the clock period).

The actual clocking of the pulse is done by putting both the phase pulse and the clock pulses into an AND gate. The output of this gate will then be the clock frequency when the phase pulse is high, or 1, and zero when the phase pulse is low. Therefore, if the output of the gate is fed into a counter, the counter will indicate the length of the phase pulse with the resolution of the clock period. (The actual output of the gate will look like figure 10 with the indicated exclusive OR "envelope" absent).

One problem with this system is that threshold devices are relied on to make square pulses from the sine wave

Figure 10

RANGE FINDER OUTPUT WAVEFORM



inputs. Thus any noise which still exists on the returned signal at this point is very likely to cause either premature or late firing of the Schmitt trigger. This will cause a corresponding phase error in that cycle of the returned signal. However, since the noise, and hence its resulting phase error, are random, the error of the final phase (i.e. range) measurement can be significantly reduced by averaging several phase differences and considering this average to be the range data for that point. This averaging is accomplished by the circuit in the lower right corner of figure 8. One output of this circuit is the third input to the phase clocking (master) AND gate. This input has the function of enabling the gate for a specified number of phase pulses and then disabling the gate until another SAMPLE command has been given.

The simplified operation of this averaging circuit is as follows. The system timer generates a SAMPLE command. To insure that the main AND gate is not enabled during the middle of a phase pulse (which would cause the first sample to be a short count), the SAMPLE command is momentarily disabled if a phase pulse is present at the AND gate input. There is therefore a minimum pulse width for the sample command, but this is not a problem. Once the existing phase pulse (if any) ends, the SAMPLE command is allowed through and it sets the RS flip-flop (the two cross coupled

NAND gates). Setting this flip-flop causes the phase clocking AND gate and the sample counter (the 3 bit counter) to be enabled. The phase pulses are now clocked and their lengths stored in the counter as described above, but now several phase pulse widths are added up in the counter. The 3 bit counter counts the number of phase pulses that are added in the main counter. Since this monitoring counter is a 3 bit counter, it will generate a carry pulse on the eighth phase pulse. This carry pulse is used to reset the RS flip-flop, thus disabling the AND gate after 8 phase lengths have been added in the main counter. Note that since a power of 2 number of samples has been added, the division required to obtain the true average pulse width (if that is what is desired), is done trivially by simply shifting the counter's binary outputs 3 bits, i.e., by moving the binary point 3 bits to the left. The carry pulse also acts as a store and clear initiating signal which tells the computer that range data is available and should be stored after which the counter should be cleared.

The eight samples that are needed can be obtained from one laser pulse, since one modulated pulse contains many cycles of the modulating waveform. The number of samples used in the averaging will, however determine the minimum width of the laser pulse. To find this minimum width briefly recall figure 9. Note that there are two

phase pulses generated for every cycle of the time expanded or down translated modulating frequency. Therefore to measure eight phase pulses, we must wait for four cycles at the lower frequency. In the system under consideration, this lower frequency is 10 KHz. Hence eight samples will take .4 milliseconds. Allowing for the laser's rise time and heterodyning stabilizing time, this indicates the laser pulse must be on the order of a millisecond.

II-e Instrumentation of the Rangefinder Electronics

The phase detection section of the rangefinder was bread-boarded in the laboratory to check its operation. Due to equipment problems the heterodyning section could not be simulated, but this will hopefully be done in the coming months by a new member of the project team (interested readers should consult next year's reports for possible results). Without the frequency translating section, the phase comparator had to be checked with a lower frequency. The time expansion feature was also lost. Phase delays of sufficient magnitudes for the comparator to resolve thus had to be artificially produced. These phase differences therefore represented no actual range measurements, but were for test purposes only.

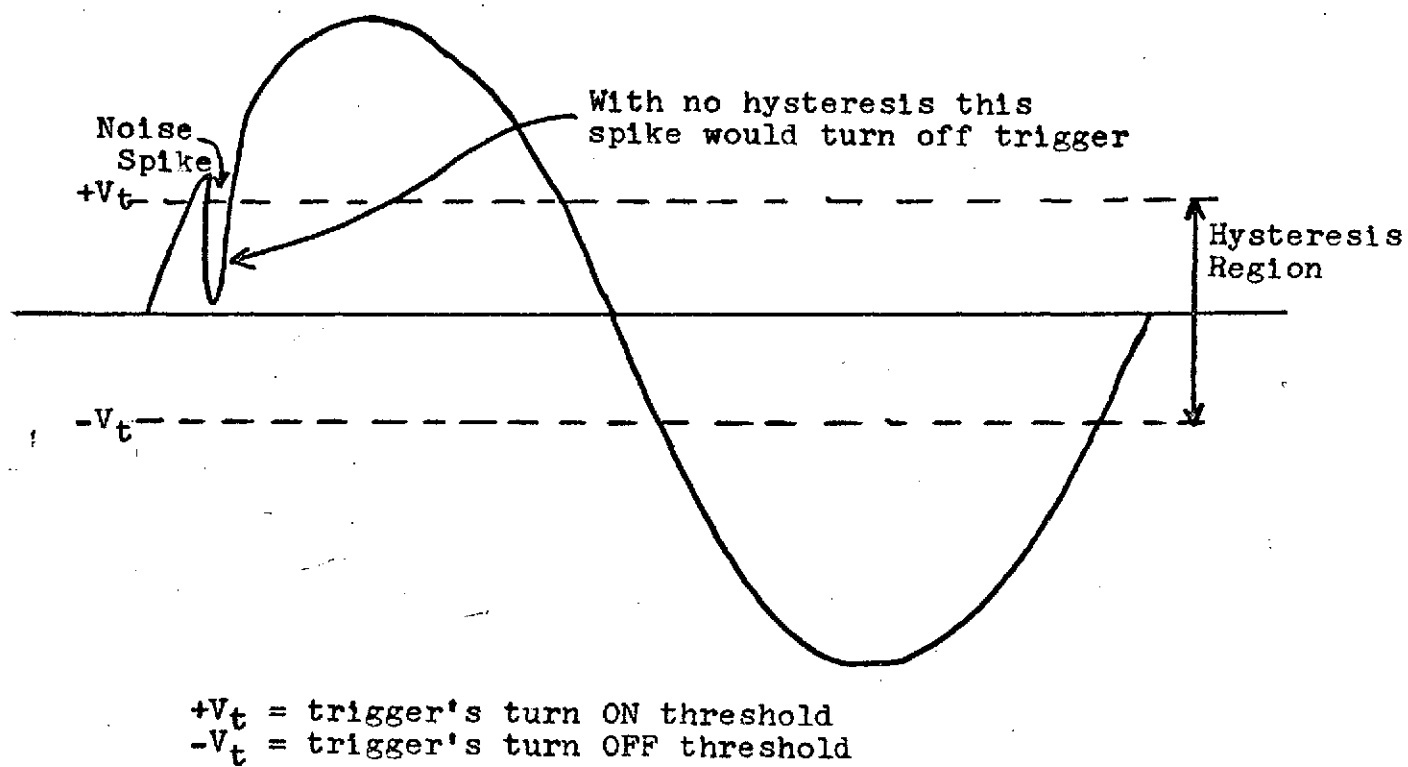
Since this self contained system had no significant noise, the Schmitt triggers were set at the more easily implemented threshold of zero with zero hysteresis (in actuality simple comparators were used). In the actual

system, more realistic values of the thresholds of say $+V_t$ and $-V_t$ should be chosen. The choice of V_t is not immediately obvious. The most logical place to locate this threshold voltage at first glance, is at the point of maximum slope of the signal, since this would reduce the sensitivity of the trigger to premature or late switching due to noise spikes close to the threshold. However for sinusoids this point is at zero voltage, which eliminates the hysteresis region and it is the hysteresis that reduces the sensitivity to premature OFF switching of the trigger after it has just crossed the ON threshold and vice versa (see figure 11). Thus the actual hysteresis, and therefore thresholds, should be set as a function of the most probable noise amplitude of the processed signal.

As for the system under test, all sections worked as expected. The output wave closely resembled figure 10 (with the exclusive OR envelope missing of course). Since NAND logic was used, however, the wave forms were inverted. With the SAMPLE command held high, the clocked phase pulses were grouped into the appropriate number of samples for averaging. Varying the phase angle of the input signals varied the phase pulse width, and therefore the number of pulses in the output count, by a proportional amount.

Figure 11

EFFECT OF SCHMITT TRIGGER ON NOISEY INPUT



CONCLUSION

A rapid scanning laser range finder was shown to be a feasible system. A non-mechanical laser scanner using either digital deflection optics or a matrix of semiconductor laser diodes was found to be the most promising method. A complete range finder scanning system was proposed around this type of rapid scan. The proposed system is highly accurate because it does not use analogue signals to determine the angles at which a laser pulse was transmitted. All directions have binary labels which correspond to angles which can be known to a high degree of accuracy.

The problem of phase blur due to the incident spot from the laser beam being distorted due to the beam's shallow angle of incidence was found to cause negligible errors compared with the accuracies desired for a reasonable range of beam diameter.

A design for a phase comparison, modulated laser range finder was proposed. Its advantages with respect to signal to noise improvement were discussed. This scheme seems to be a very promising way of achieving the desired ± 1 centimeter accuracy at mid-range (≈ 15 to 20 meters).

A section of the design was bread-boarded and tested. The tests were in good agreement with predicted results. But future work should be done to complete the laboratory testing of the entire system. Work is continuing in this area currently.

REFERENCES

- [1] Fowler, V. J. and J. Schafer, "A Survey of Laser Beam Deflection Techniques", Proceedings of the IEEE, Vol. 54, no. 10, October 1966, pp 1437-1443.
- [2] Advertisement by Coherent Optics Inc., Laser Focus, Feb. 1970, pp 13.
- [3] Kulcke, W., et. al., "Digital Light Deflectors", Proceedings of the IEEE, Vol. 54, no. 10, Oct. 1966, pp 1419-1429.
- [4] Nelson, T. J., "Digital Light Deflection", Bell System Technical Journal, Vol. 43, no. 3, May 1964, pp 821-845.
- [5] Kuriger, William, "A Proposed Obstacle Sensor for a Mars Rover", Journal of Spacecraft and Rockets, Vol. 8, no. 10, October 1971, pp 1043-1048.
- [6] Nikon Lens Catalogue, Nippon Kogaku K.K. (Company).